DISCOVERY OF FOUR DOUBLY IMAGED QUASAR LENSES FROM THE SLOAN DIGITAL SKY SURVEY

Naohisa Inada[1], Masamune Oguri[2,3], Cristian E. Rusu[4,5], Issha Kayo[6,7], and Tomoki Morokuma[8]

[1] Department of Physics, Nara National College of Technology, Yamatokohriyama, Nara 639-1080, Japan
[2] Department of Physics, Graduate School of Science, University of Tokyo, Hongo 7-3-1, Bunkyo-ku, Tokyo 113-0033, Japan
[3] Kavli Institute for the Physics and Mathematics of the Universe, The University of Tokyo, 5-1-5 Kashiwa-no-ha, Kashiwa, Chiba 277-8568, Japan
[4] Optical and Infrared Astronomy Division, National Astronomical Observatory of Japan, 2-21-1, Osawa, Mitaka, Tokyo 181-8588, Japan
[5] Department of Astronomy, Graduate School of Science, University of Tokyo 7-3-1, Hongo Bunkyo-ku, Tokyo 113-0033, Japan
[6] Department of Physics, Toho University, Funabashi, Chiba 274-8510, Japan
[7] Department of Liberal Arts, Tokyo University of Technology, 5-23-22, Nishikamata, Ota-ku, Tokyo 144-8650, Japan
[8] Institute of Astronomy, Faculty of Science, University of Tokyo, 2-21-1 Osawa, Mitaka, Tokyo 181-0015, Japan

ABSTRACT

We report the discovery of four doubly imaged quasar lenses. All the four systems are selected as lensed quasar candidates from the Sloan Digital Sky Survey data. We confirm their lensing hypothesis with additional imaging and spectroscopic follow-up observations. The discovered lenses are SDSS J0743+2457 with the source redshift $z_s = 2.165$, the lens redshift $z_l = 0.381$, and the image separation $\theta = 1{.}''034$, SDSS J1128+2402 with $z_s = 1.608$ and $\theta = 0{.}''844$, SDSS J1405+0959 with $z_s = 1.810$, $z_l \approx 0.66$, and $\theta = 1{.}''978$, and SDSS J1515+1511 with $z_s = 2.054$, $z_l = 0.742$, and $\theta = 1{.}''989$. It is difficult to estimate the lens redshift of SDSS J1128+2402 from the current data. Two of the four systems (SDSS J1405+0959 and SDSS J1515+1511) are included in our final statistical lens sample to derive constraints on dark energy and the evolution of massive galaxies.

Key words: gravitational lensing: strong – quasars: general

Online-only material: supplemental data

1. INTRODUCTION

Gravitationally lensed quasars have proven to be a useful tool for a variety of astrophysical and cosmological studies, as described e.g., in Kochanek (2006). Applications of quasar lenses include constraints on cosmological parameters and measurements of mass distributions for galaxy- and cluster-scale halos, interstellar medium associated with lensing or intervening galaxies, and the structure of quasar accretion disk and outflow (e.g., Fukugita et al. 1990; Kochanek 1991; Oguri et al. 2013; Curran et al. 2007; Poindexter et al. 2008; Misawa et al. 2013). The use of these quasar lenses can be enhanced by constructing a homogeneous lens sample with a well-characterized selection function. For instance, the Cosmic Lens All Sky Survey (Myers et al. 2003; Browne et al. 2003) has provided a complete sample of 22 strong lenses selected among $\sim$16,000 radio sources, which has been used for a number of cosmological and astrophysical studies (e.g., Chae et al. 2006). Currently, we have completed the SDSS Quasar Lens Search (SQLS; Oguri et al. 2006), which is the current largest lensed quasar survey using optical data of the Sloan Digital Sky Survey (SDSS; York et al. 2000). The total number of lensed quasars identified in the SDSS data is 62[9] (Inada et al. 2012). The statistical analysis for SQLS lenses to constrain both cosmological parameters and the evolution of massive galaxies has been reported in Oguri et al. (2012).

In this paper, we report the discovery of four lensed quasars from the SQLS. Since the description of the four lensed quasars in Inada et al. (2012) is so brief, we show the detailed properties of the four systems here. We briefly describe the SDSS data and our algorithm to locate lensed quasar candidates in Section 2. We then present follow-up observations to confirm their lensing

hypotheses in Section 3. We carry out mass modeling in Section 4. Our result is summarized in Section 5.

2. CANDIDATE SELECTION FROM THE SLOAN DIGITAL SKY SURVEY

The SQLS identifies lensed quasars among $\sim$100,000 quasars (Schneider et al. 2010) from the SDSS Data Release 7 (DR7). The SDSS is a survey using a dedicated wide-field 2.5 m telescope (Gunn et al. 2006) at the Apache Point Observatory (New Mexico, USA) to conduct imaging and spectroscopic surveys for a quarter of the sky. The imaging data were obtained through five broad-band filters (*ugriz*; Fukugita et al. 1996; Gunn et al. 1998; Doi et al. 2010) with astrometric accuracy better than $\sim 0{.}''1$ (Pier et al. 2003) and with photometric zeropoint accuracy better than $\sim$0.01 mag (Hogg et al. 2001; Smith et al. 2002; Ivezić et al. 2004; Tucker et al. 2006; Padmanabhan et al. 2008). Quasar and galaxy candidates were selected by the SDSS spectroscopic pipeline based on the imaging data (Eisenstein et al. 2001; Richards et al. 2002; Strauss et al. 2002). The candidates were tiled in each plate according to the algorithm of Blanton et al. (2003), and were observed with multi-object fiber spectrographs ($R \sim 1800$) covering 3800–9200 Å (Blanton et al. 2003). The SDSS DR7 data have already been made public (Stoughton et al. 2002; Abazajian et al. 2003, 2004, 2005, 2009; Adelman-McCarthy et al. 2006, 2007, 2008).

The procedure to identify lensed quasar candidates from the spectroscopic SDSS quasars has been described in the series of SQLS papers (e.g., Inada et al. 2008), which we outline here. We use two selection methods. One is to find quasars with nearby objects whose colors are similar to the quasars. This method is tagged as the "color selection." The color selection does not always work well for the SDSS data because of the relatively poor spatial resolution of SDSS imaging data, whose seeing sizes are comparable to typical image separations of

---

[9] The gravitational lens nature of an object is not secure (Rusu et al. 2013).

Table 1
SDSS Properties of the Lens Systems

Object	R.A. (J2000)	Decl. (J2000)	u	g	r	i	z	Redshift
SDSS J0743+2457	07:43:52.61	+24:57:43.6	19.92 ± 0.04	19.42 ± 0.02	19.19 ± 0.02	19.09 ± 0.02	18.76 ± 0.04	2.165
SDSS J1128+2402	11:28:18.49	+24:02:17.4	18.35 ± 0.02	18.30 ± 0.02	18.12 ± 0.02	17.92 ± 0.01	17.92 ± 0.02	1.608
SDSS J1405+0959	14:05:15.42	+09:59:31.3	19.97 ± 0.06	19.62 ± 0.04	19.48 ± 0.03	19.10 ± 0.04	19.19 ± 0.06	1.810
	14:05:15.40	+09:59:29.3	20.67 ± 0.15	20.52 ± 0.13	20.31 ± 0.09	19.72 ± 0.09	19.50 ± 0.12	. . .
SDSS J1515+1511	15:15:38.59	+15:11:35.8	18.43 ± 0.04	18.27 ± 0.04	18.23 ± 0.04	18.11 ± 0.04	17.91 ± 0.04	2.054
	15:15:38.47	+15:11:34.7	18.94 ± 0.09	18.70 ± 0.08	18.61 ± 0.07	18.37 ± 0.07	18.19 ± 0.07	. . .

Table 2
Summary of Imaging Follow-up Observations

Object	Instruments	Observing Date (UT)	Exposure (s)
SDSS J0743+2457	Tek2k($VRIz$)	2010 Jan 16(V), 2009 Apr 16(R), 2010 Jan 17(Iz)	720(V), 300(R), 960(Iz)
SDSS J1128+2402	Tek2k(VI)	2007 Apr 12(V), 2010 Jan 17(I)	300(V), 960(I)
SDSS J1405+0959	UH8k(VI), Tek2k(R)	2006 Mar 25(VI), 2009 Apr 16(R)	270(V), 400(R), 450(I)
SDSS J1515+1511	Tek2k(I), S-cam(i), IRCS(K'), SPIcam(z)	2009 Apr 16(I), 2011 Mar 31(i), 2011 May 7(K'), 2011 Mar 26(z)	400(I), 90(i), 1320(K'), 1080(z)

Notes. The Tektronix 2048 × 2048 CCD camera (Tek2k) and the UH8k wide-field imager (UH8k) are installed on the UH88 telescope. The Suprime-Cam (S-cam; Miyazaki et al. 2002) and the Infrared Camera and Spectrograph (IRCS; Kobayashi et al. 2000) are installed on the Subaru telescope. The Seaver Prototype Imaging camera (SPIcam) is installed on the ARC telescope.
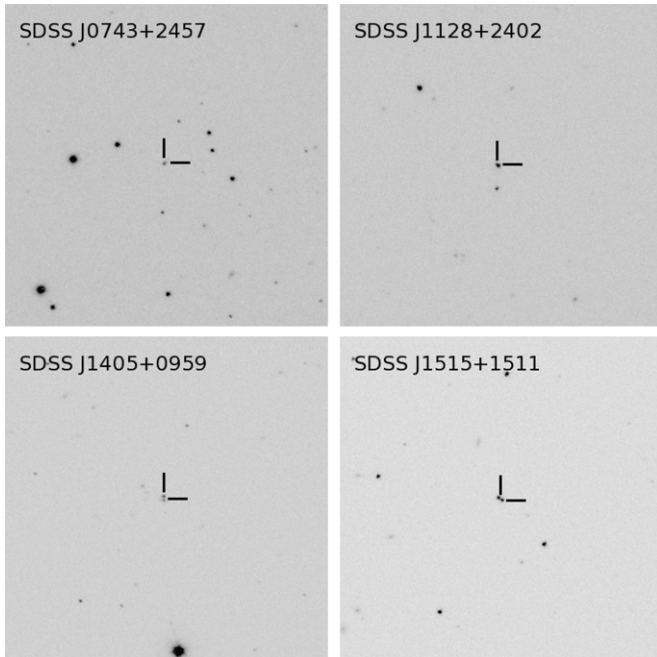

Figure 1. Finding charts (SDSS i-band images) of the four lens systems. The size of each figure is $2.''5 \times 2.''5$. North is up and east is left.

quasar lenses. Therefore, in order to find lenses which are not deblended into multiple components in the SDSS data, we also exploit the so-called morphological selection, in which we select spectroscopic quasars with extended morphologies as lensed quasar candidates. SDSS J0743+2457 and SDSS J1128+2402 are selected by the morphological selection, whereas SDSS J1405+0959 and SDSS J1515+1511 are selected by both the color selection and the morphological selection. The SDSS properties of these four candidates are summarized in Table 1. We also show the SDSS i-band images of the four objects in Figure 1.

We note that SDSS J0743+2457 and SDSS J1405+0959 have been reported as quasar lenses ULAS 074352.6+245743 and ULAS 140515.4+095931, respectively, by the Major UKIDSS-SDSS Cosmic Lens Survey (MUSCLES) survey (Jackson et al. 2012). In the MUSCLES survey lens candidates are selected by cross-matching SDSS quasars with UKIDSS near-infrared images which typically have much better spatial resolution. Our identification of SDSS J0743+2457 and SDSS J1405+0959 as lens candidates is independent of the MUSCLES survey result.

3. FOLLOW-UP IMAGING AND SPECTROSCOPY

3.1. Follow-up Data

We carried out follow-up imaging and spectroscopic observations using the University of Hawaii 2.2 m telescope (UH88), the Astrophysical Research Consortium 3.5 m telescope (ARC), the 3.58 m Telescopio Nazionale Galileo (TNG), the Subaru 8.2 m telescope, and the Gemini North 8.1 m telescope, to confirm the lensing hypothesis of the four lensed quasar candidates. All the four candidates are doubly imaged lens candidates, and therefore their lensing hypothesis should be confirmed by both similar spectral energy distributions (SEDs) for the two stellar components and the existence of an extended object between the two components that act as a lens. We summarize the details of our follow-up imaging and spectroscopic observations in Tables 2 and 3.

We clearly detect two stellar components in each original image of the follow-up imaging observations. Once we subtract two point spread functions (PSFs) using GALFIT (Peng et al. 2002), we detect a significant residual, indicating an additional component in between the two PSFs, for all four systems. We then model the system with two PSFs plus an extended component represented by a Sérsic profile. As shown in Figure 2, an extended component is clearly visible after subtracting the two PSFs. The Sérsic parameters of the best-fitting model are summarized in Table 4. We also summarize the astrometric and photometric results for each system in Table 5.
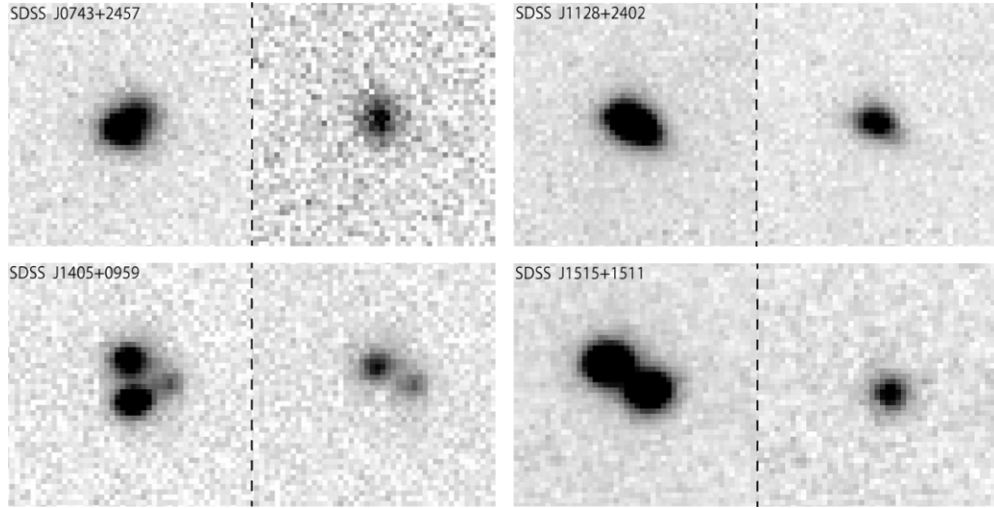
Figure 2. Follow-up *I*-band images of the four lens systems. The images of SDSS J0743+2457, SDSS J1128+2402, and SDSS J1515+1511 were taken with UH88/Tek2k (0″.22 pixel^{-1}), and the image of SDSS J1405+0959 were taken with UH88/8k (0″.235 pixel^{-1}). North is up and east is left. For each system, the left panel shows the original image and the right panel shows the image after subtracting two PSF components. The residuals in the right panels are all fitted well by the Sérsic profile. See Table 4 for the fitting results.

Table 3
Summary of Spectroscopic Follow-up Observations

Object	Instrument	Slit Width	Filter/Grism	Wavelength Coverage (Å)	Observing Date (UT)	Exposure (s)
SDSS J0743+2457	GMOS	1″	GG455/R150	4600–9000	2010 Mar 22	1200
SDSS J1128+2402	GMOS	1″	GG455/R150	4600–9000	2010 Mar 22	900
SDSS J1405+0959	DOLORES	1″	LR-B	3700–7800	2008 Mar 1	1800
SDSS J1515+1511	DOLORES	1″	LR-B	3700–7800	2008 Apr 13	900

Notes. The Gemini Multi-Object Spectrograph (GMOS) is installed on the Gemini telescope (North). The Device Optimized for the LOw RESolution (DOLORES) is installed on the TNG telescope.

Table 4
Sérsic Parameters of the Lensing Galaxies

Object	r_e[a] (″)	n[b]	e[c]	θ_e[c] (°)
SDSS J0743+2457	0.58 ± 0.24	0.71 ± 0.85	0.47 ± 0.16	6.48 ± 14.65
SDSS J1128+2402	0.33 ± 0.06	1.79 ± 0.50	0.49 ± 0.03	56.03 ± 3.56
SDSS J1405+0959	0.37 ± 0.05	2.15 ± 0.77	0.06 ± 0.11	−17.02 ± 81.33
SDSS J1515+1511	1.06 ± 0.08	1.08 ± 0.20	0.53 ± 0.03	−16.20 ± 2.50

Notes. Best-fitting Sérsic parameters measured in the *I*-band images with GALFIT (the parameters for SDSS J1515+1511 are measured in the *i*-band. The Subaru S-cam *i*-band image has smaller seeing).
[a] Effective radius (in arcsec) of the Sérsic profile.
[b] Sérsic concentration index.
[c] Ellipticity and position angle measured east of north.

Results of the spectroscopic follow-up observations are shown in Figure 3. For each candidate, we aligned the slit direction such that we can observe the two stellar components simultaneously. The good seeing condition (FWHM ≲ 1″.0) enabled us to extract the spectrum of each component easily using standard IRAF[10] tasks. The spectra indicate that the SEDs of the two stellar components are quite similar for all four systems. In particular, the two quasar components of the SDSS J1405+0959 system have very similar broad absorption, which is in strong support of strong lensing interpretation of this system.

The fainter component of SDSS J1515+1511 shows a strong Mg II absorption at ∼5900 Å, which corresponds to an absorber at $z = 0.742$, and is likely to be associated with the lensing galaxy (see below).

3.2. Lens Redshifts

First we examine our follow-up spectra carefully to look for any spectral signature of lensing galaxies. We find that the spectrum of the fainter component of SDSS J0743+2457 contains a significant amount of galaxy flux. We extract the spectrum of the lensing galaxy G by subtracting the spectrum of image A, with an appropriate offset corresponding to the flux ratio, from that of image B. Figure 4 clearly indicates that the lensing galaxy is an early-type galaxy at $z_l = 0.381$.

---

[10] IRAF is distributed by the National Optical Astronomy Observatories, which are operated by the Association of Universities for Research in Astronomy, Inc., under cooperative agreement with the National Science Foundation.
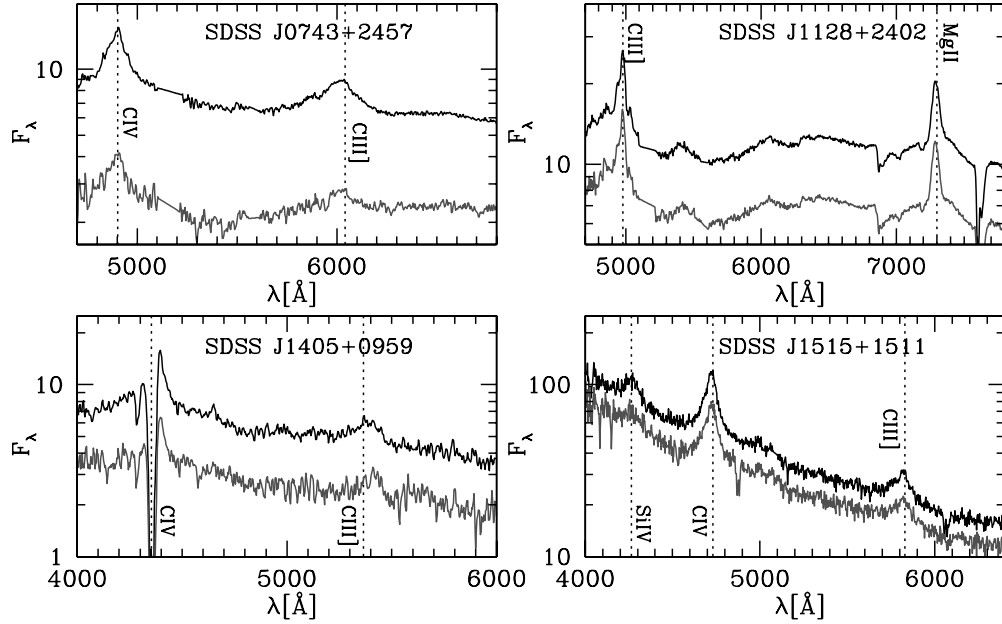
Figure 3. Spectra of two lensed quasar images. The data between 5100 Å and 5200 Å for SDSS J0743+2457 and SDSS J1128+2402 are excluded due to a gap of the detector. The wavelengths of quasar emission lines are indicated by vertical dotted lines. See Table 3 for details of our spectroscopic follow-up observations.

(Supplemental data of this figure are available in the online journal.)

Table 5
Relative Astrometry and Photometry of the Lens Systems

Object	ΔX (arcsec)	ΔY (arcsec)	V	R	I
		SDSS J0743+2457 ($\theta = 1\rlap{.}''034 \pm 0\rlap{.}''056$)			
A	$\equiv 0.000$	$\equiv 0.000$	19.33 ± 0.01	19.14 ± 0.01	18.90 ± 0.02
B	-0.796 ± 0.040	-0.660 ± 0.040	21.03 ± 0.06	20.53 ± 0.02	20.36 ± 0.31
G	-0.590 ± 0.070	-0.546 ± 0.070	$\dots$	$\dots$	20.47 ± 0.37
		SDSS J1128+2402 ($\theta = 0\rlap{.}''844 \pm 0\rlap{.}''006$)			
A	$\equiv 0.000$	$\equiv 0.000$	18.55 ± 0.01	$\dots$	18.48 ± 0.02
B	-0.669 ± 0.004	0.515 ± 0.004	19.38 ± 0.01	$\dots$	19.15 ± 0.03
G	-0.429 ± 0.007	0.361 ± 0.007	21.74 ± 0.25	$\dots$	18.56 ± 0.06
		SDSS J1405+0959 ($\theta = 1\rlap{.}''978 \pm 0\rlap{.}''013$)			
A	$\equiv 0.000$	$\equiv 0.000$	19.34 ± 0.01	19.18 ± 0.01	18.71 ± 0.01
B	0.282 ± 0.009	-1.958 ± 0.009	20.43 ± 0.01	20.22 ± 0.04	19.90 ± 0.05
G1	0.021 ± 0.021	-1.614 ± 0.021	22.42 ± 0.20	20.59 ± 0.04	19.70 ± 0.05
G2	-1.553 ± 0.024	-0.792 ± 0.024	22.51 ± 0.67	21.25 ± 0.09	20.53 ± 0.10
		SDSS J1515+1511 ($\theta = 1\rlap{.}''989 \pm 0\rlap{.}''0.003$)			
A	$\equiv 0.000$	$\equiv 0.000$	$i = 18.15 \pm 0.01$	$z = 17.89 \pm 0.01$	$K' = 15.80 \pm 0.01$
B	1.648 ± 0.002	-1.114 ± 0.002	$i = 18.54 \pm 0.01$	$z = 18.32 \pm 0.02$	$K' = 16.06 \pm 0.01$
G	1.384 ± 0.030	-0.946 ± 0.036	$i = 21.39 \pm 0.06$	$z = 20.73 \pm 0.51$	$K' = 17.03 \pm 0.04$

Notes. Magnitudes are in the Vega system, except for i- and z-band which are in AB system. The K' band photometric zero point for SDSS J1515+1511 is less robust, as it is based on a single star in the field of view (non-photometric conditions), with catalog uncertainty 0.11 mag.

For the other lens systems, we estimate redshifts of the lensing galaxies based on their colors. For SDSS J1405+0959, the Sérsic concentration index suggests that the residual may be a late-type galaxy. In this case, the $V - R$ and $R - I$ colors imply that the redshift is $z_l \sim 0.5$ (e.g., Fukugita et al. 1995). This is broadly consistent with $z_l \sim 0.66$ derived in Jackson et al. (2012) using the overall spectral shape of the lensing galaxy in their follow-up spectroscopic data. For SDSS J1515+1511, the morphology is more robust in the i-band, where it is consistent with a late-type galaxy. Its color $i - K' \sim 4.4$ implies the redshift of $z \sim 0.8$–1.1, which is close to the redshift $z = 0.742$ of the

strong absorber seen in the spectrum of the fainter quasar image. Thus we tentatively assign its lens redshift to be $z_l = 0.742$. It is difficult to estimate the photometric lens redshift of SDSS J1128+2402 from the current data.

4. MASS MODELING

We model the lens systems adopting a singular isothermal ellipsoid mass model using *glafic* (Oguri 2010). The number of parameters is eight (the position and flux of the source quasar, the position of the lensing galaxy, the Einstein radius,
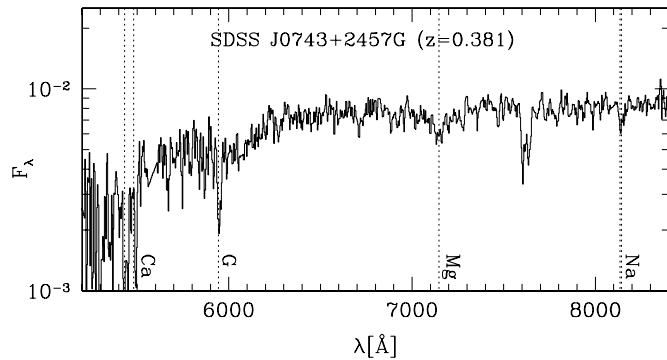
Figure 4. Spectrum of the lensing galaxy G of SDSS J0743+2457. The spectrum clearly indicates that the lensing galaxy is an early-type galaxy at $z = 0.381$.

(Supplemental data of this figure are available in the online journal.)

Table 6
Results of Mass Modeling

Object	R_E[a] ('')	e[b]	θ_e[b] (°)	μ_{tot}[c]
SDSS J0743+2457	0.53	0.19	89.4	3.6
SDSS J1128+2402	0.42	0.06	−75.4	6.0
SDSS J1405+0959	1.03	0.49	67.4	2.6
SDSS J1515+1511	0.90	0.60	−25.0	2.8

Notes.
[a] Einstein radius in arcsec.
[b] Ellipticity and position angle measured east of north.
[c] Total magnification factor predicted by the best fitting model.

the ellipticity, and the position angle), while the number of constraints from the imaging observations is also eight (the positions and fluxes of the two quasar components, and the position of the lensing galaxy). Thus the model has zero degrees of freedom. We adopt the *I*-band imaging result as constraints for SDSS J0743+2457, SDSS J1128+2402, and SDSS J1405+0959. For SDSS J1515+1511, we use the *i*-band imaging result in spite of the lens being comparatively fainter, because the seeing was smaller, there were more stars available to build a PSF, and both astrometry and morphology are more robust. We summarize the parameters of the best-fitting ($\chi^2 \sim 0$) models in Table 6. As is common (e.g., Keeton et al. 1998), there are large differences in the lensing galaxy shapes between the observations (Table 4) and the best-fitting mass model parameters (Table 6). This may partly be explained by nearby perturbers which affect the lens potentials.

5. SUMMARY

We have confirmed the lensing hypothesis for four lens candidates selected by the SQLS, based on the similar SEDs of the stellar components together with the existence of extended objects in between the stellar components, and the successful mass modeling of the observed configurations. All four are doubly imaged quasar lens systems: SDSS J0743+2457 ($z_s = 2.165, z_l = 0.381, \theta = 1''034$), SDSS J1128+2402 ($z_s = 1.608, \theta = 0''844$), SDSS J1405+0959 ($z_s = 1.810, z_l \sim 0.66, \theta = 1''978$), and SDSS J1515+1511 ($z_s = 2.054, z_l = 0.742, \theta = 1''989$). Two of them (SDSS J1405+0959 and SDSS J1515+1511) are included in the SQLS statistical sample (Inada et al. 2012) and are used for cosmological constraints (Oguri et al. 2012).

These lens systems represent likely the last quasar lenses to emerge from the SQLS project. The applications of the SQLS lenses have been limited by the lack of high-resolution images for many of the SQLS lenses. We are therefore currently conducting a program to observe the SQLS lenses with Subaru telescope laser guide start adaptive optics system to accurately measure the quasar image positions and light profile of the lensing galaxy (Rusu et al. 2011; C. E. Rusu et al., in preparation). We are also carrying out a lensed quasar survey using the SDSS-III data (Eisenstein et al. 2011) from which we will be able to discover more quasar lenses.

REFERENCES

Abazajian, K., Adelman-McCarthy, J. K., Agüeros, M. A., et al. 2003, AJ, 126, 2081
Abazajian, K., Adelman-McCarthy, J. K., Agüeros, M. A., et al. 2004, AJ, 128, 502

Abazajian, K., Adelman-McCarthy, J. K., Agüeros, M. A., et al. 2005, AJ, 129, 1755
Abazajian, K. N., Adelman-McCarthy, J. K., Agüeros, M. A., et al. 2009, ApJS, 182, 543
Adelman-McCarthy, J. K., Agüeros, M. A., Allam, S. S., et al. 2006, ApJS, 162, 38
Adelman-McCarthy, J. K., Agüeros, M. A., Allam, S. S., et al. 2007, ApJS, 172, 634
Adelman-McCarthy, J. K., Agüeros, M. A., Allam, S. S., et al. 2008, ApJS, 175, 297
Blanton, M. R., Lin, H., Lupton, R. H., et al. 2003, AJ, 125, 2276
Browne, I. W. A., Wilkinson, P. N., Jackson, N. J. F., et al. 2003, MNRAS, 341, 13
Chae, K.-H., Mao, S., & Kang, X. 2006, MNRAS, 373, 1369
Curran, S. J., Darling, J., Bolatto, A. D., et al. 2007, MNRAS, 382, L11
Doi, M., Tanaka, M., Fukugita, M., et al. 2010, AJ, 139, 1628
Eisenstein, D. J., Annis, J., Gunn, J. E., et al. 2001, AJ, 122, 2267
Eisenstein, D. J., Weinberg, D. H., Agol, E., et al. 2011, AJ, 142, 72
Fukugita, M., Futamase, T., & Kasai, M. 1990, MNRAS, 246, 24
Fukugita, M., Ichikawa, T., Gunn, J. E., et al. 1996, AJ, 111, 1748
Fukugita, M., Shimasaku, K., & Ichikawa, T. 1995, PASP, 107, 945
Gunn, J. E., Carr, M., Rockosi, C., et al. 1998, AJ, 116, 3040
Gunn, J. E., Siegmund, W. A., Mannery, E. J., et al. 2006, AJ, 131, 2332
Hogg, D. W., Finkbeiner, D. P., Schlegel, D. J., & Gunn, J. E. 2001, AJ, 122, 2129
Inada, N., Oguri, M., Becker, R. H., et al. 2008, AJ, 135, 496
Inada, N., Oguri, M., Shin, M.-S., et al. 2012, AJ, 143, 119
Ivezić, Ž., Lupton, R. H., Schlegel, D., et al. 2004, AN, 325, 583

Jackson, N., Rampadarath, H., Ofek, E. O., Oguri, M., & Shin, M.-S. 2012, MNRAS, 419, 2014
Keeton, C. R., Kochanek, C. S., & Falco, E. E. 1998, ApJ, 509, 561
Kobayashi, N., Tokunaga, A. T., Terada, H., et al. 2000, Proc. SPIE, 4008, 1056
Kochanek, C. S. 1991, ApJ, 373, 354
Kochanek, C. S., Schneider, P., & Wambsganss, J. 2006, in Proc. 33rd Saas-Fee Advanced Course, Part 2 of Gravitational Lensing: Strong, Weak & Micro, ed. G. Meylan, P. Jetzer, & P. North (Berlin: Springer), 91
Misawa, T., Inada, N., Ohsuga, K., et al. 2013, AJ, 145, 48
Miyazaki, S., Komiyama, Y., Sekiguchi, M., et al. 2002, PASJ, 54, 833
Myers, S. T., Jackson, N. J., Browne, I. W. A., et al. 2003, MNRAS, 341, 1
Oguri, M. 2010, PASJ, 62, 1017
Oguri, M., Inada, N., Pindor, B., et al. 2006, AJ, 132, 999
Oguri, M., Inada, N., Strauss, M. A., et al. 2012, AJ, 143, 120
Oguri, M., Schrabback, T., Jullo, E., et al. 2013, MNRAS, 429, 482
Padmanabhan, N., Schlegel, D. J., Finkbeiner, D. P., et al. 2008, ApJ, 674, 1217
Peng, C. Y., Ho, L. C., Impey, C. D., & Rix, H.-W. 2002, AJ, 124, 266
Pier, J. R., Munn, J. A., Hindsley, R. B., et al. 2003, AJ, 125, 1559
Poindexter, S., Morgan, N., & Kochanek, C. S. 2008, ApJ, 673, 34
Richards, G. T., Fan, X., Newberg, H. J., et al. 2002, AJ, 123, 2945
Rusu, C. E., Oguri, M., Inada, N., et al. 2011, ApJ, 738, 30
Rusu, C. E., Oguri, M., Iye, M., et al. 2013, ApJ, 765, 139
Schneider, D. P., Richards, G. T., Hall, P. B., et al. 2010, AJ, 139, 2360
Smith, J. A., Tucker, D. L., Kent, S., et al. 2002, AJ, 123, 2121
Stoughton, C., Lupton, R. H., Bernardi, M., et al. 2002, AJ, 123, 485
Strauss, M. A., Weinberg, D. H., Lupton, R. H., et al. 2002, AJ, 124, 1810
Tucker, D. L., Kent, S., Richmond, M. W., et al. 2006, AN, 327, 821
York, D. G., Adelman, J., Anderson, J. E., Jr., et al. 2000, AJ, 120, 1579

ERRATUM: "DISCOVERY OF FOUR DOUBLY IMAGED QUASAR LENSES FROM THE SLOAN DIGITAL SKY SURVEY" (2014, AJ, 147, 153)

Naohisa Inada[1], Masamune Oguri[2,3], Cristian E. Rusu[4,5], Issha Kayo[6,7], and Tomoki Morokuma[8]
[1] Department of Physics, Nara National College of Technology, Yamatokohriyama, Nara 639-1080, Japan
[2] Department of Physics, Graduate School of Science, University of Tokyo, Hongo 7-3-1, Bunkyo-ku, Tokyo 113-0033, Japan
[3] Kavli Institute for the Physics and Mathematics of the Universe, The University of Tokyo, 5-1-5 Kashiwa-no-ha, Kashiwa, Chiba 277-8568, Japan
[4] Optical and Infrared Astronomy Division, National Astronomical Observatory of Japan, 2-21-1, Osawa, Mitaka, Tokyo 181-8588, Japan
[5] Department of Astronomy, Graduate School of Science, University of Tokyo 7-3-1, Hongo Bunkyo-ku, Tokyo 113-0033, Japan
[6] Department of Physics, Toho University, Funabashi, Chiba 274-8510, Japan
[7] Department of Liberal Arts, Tokyo University of Technology, 5-23-22, Nishikamata, Ota-ku, Tokyo 144-8650, Japan
[8] Institute of Astronomy, Faculty of Science, University of Tokyo, 2-21-1 Osawa, Mitaka, Tokyo 181-0015, Japan
Received 2014 September 26; accepted 2014 October 9; published 2015 January 5

As shown in Table 5 of the paper, South is up and West is left just for the original and subtracted images of SDSS 1405+0959 (lower left panel) in Figure 2. We apologize for the inconvenience, although this error does not affect the conclusion of the paper. See Rusu et al. (2014) for the detailed observation of SDSS 1405+0959.

REFERENCES

Rusu, C. E., Oguri, M., Minowa, Y., et al. 2014, MNRAS, 444, 2561